

## Peptide salt bridge stability: From gas phase via microhydration to bulk water simulations

Eva Pluhařová,<sup>1,a)</sup> Ondrej Marsalek,<sup>1,b)</sup> Burkhard Schmidt,<sup>2,c)</sup> and Pavel Jungwirth<sup>1,d)</sup>

<sup>1</sup>*Institute of Organic Chemistry and Biochemistry, Academy of Sciences of the Czech Republic, Flemingovo náměstí 2, Prague 6, CZ-16610, Czech Republic*

<sup>2</sup>*Institut für Mathematik, Freie Universität Berlin, Arnimallee 6, D-14195 Berlin, Germany*

(Received 12 July 2012; accepted 17 October 2012; published online 8 November 2012)

The salt bridge formation and stability in the terminated lysine-glutamate dipeptide is investigated in water clusters of increasing size up to the limit of bulk water. Proton transfer dynamics between the acidic and basic side chains is described by DFT-based Born-Oppenheimer molecular dynamics simulations. While the desolvated peptide prefers to be in its neutral state, already the addition of a single water molecule can trigger proton transfer from the glutamate side chain to the lysine side chain, leading to a zwitterionic salt bridge state. Upon adding more water molecules we find that stabilization of the zwitterionic state critically depends on the number of hydrogen bonds between side chain termini, the water molecules, and the peptidic backbone. Employing classical molecular dynamics simulations for larger clusters, we observed that the salt bridge is weakened upon additional hydration. Consequently, long-lived solvent shared ion pairs are observed for about 30 water molecules while solvent separated ion pairs are found when at least 40 or more water molecules hydrate the dipeptide. These results have implications for the formation and stability of salt bridges at partially dehydrated surfaces of aqueous proteins. © 2012 American Institute of Physics. [<http://dx.doi.org/10.1063/1.4765052>]

### I. INTRODUCTION

In proteins, salt bridges are the most prominent non-covalent interactions occurring between titratable amino acid side chains, typically an acidic group and a basic group in water.<sup>1</sup> Prototypical examples of the former ones are the carboxylate group of Glu and Asp, while the latter ones are represented by the ammonium group of Lys, and the guanidinium group of Arg. Whereas the oppositely charged groups attract each other, there is also a tendency for water to solvate these charges separately, thereby shielding them to a certain extent. Situations ranging from a contact ion pair (salt bridge) over a solvent shared ion pair (with a shared bridging water molecule) to a solvent separated ion pair (where more than one solvent molecule form a bridge between the charge centers) to completely separately solvated ionic groups can occur. This indicates that the stability of the salt bridge is just a few  $k_B T$  at best. There is, therefore, discussion about the relative importance of salt bridges in stabilizing protein structure based on experimental results,<sup>2–5</sup> database studies,<sup>2,6</sup> as well as theoretical modeling.<sup>7–9</sup> It has been shown that particularly strong salt bridges are formed for (partially) buried residues.<sup>10</sup> Although the acidic and basic side chain groups most often appear at the outer protein surface, the amount of charged residues found buried deeper inside the protein is non-negligible.<sup>2,6,10–13</sup>

In the former case, the two groups are exposed to water, and the Coulomb interaction between them is dramatically weakened by interactions with solvent molecules. In the latter case of (partially) embedded side chains the salt bridge can become stronger due to the lowering of the effective dielectric constant, however, the possibility of a neutralizing proton transfer between the chains needs to be taken into consideration, too. It is, therefore, of considerable interest to explore how interactions between acidic and basic side chains change as one adds solvent molecules, moving from the situation pertinent to desolvated side chains to the aqueous bulk phase.

Building up the solvent environment in a stepwise fashion allows to address the question of how many solvent molecules are needed to observe the proton transfer between titratable side chains (proceeding either directly or through protons hopping between neighboring water molecules) moving thus from two neutral side chains to a pair of a oppositely charged ionic groups forming a salt bridge. A subsequent question is how the strength of the salt bridge changes upon gradual addition of water molecules. Hence, in our present work we focus on two hydration regimes. In the first one, we study systems with a small number of water molecules focusing on the interplay between neutral and ionized forms of the titratable side chains. The related phenomenon of the emergence of the zwitterionic state has been extensively studied in the case of single amino acids, where the  $-NH_2$  and  $-COOH$  groups are involved, analogously to the situation of a Lys-Gly or Lys-Asp side chains.<sup>14–19</sup> The second regime investigated in the present work deals with higher degrees of hydration. Once the salt bridge is formed in the microhydrated environment, upon further addition of water molecules the protonation state of the side chains remains the same,

<sup>a)</sup> Author to whom correspondence should be addressed. [eva.pluharova@uochb.cas.cz](mailto:eva.pluharova@uochb.cas.cz).

<sup>b)</sup> [ondrej.marsalek@uochb.cas.cz](mailto:ondrej.marsalek@uochb.cas.cz).

<sup>c)</sup> [burkhard.schmidt@fu-berlin.de](mailto:burkhard.schmidt@fu-berlin.de).

<sup>d)</sup> [pavel.jungwirth@uochb.cas.cz](mailto:pavel.jungwirth@uochb.cas.cz).

but the salt bridge becomes progressively weakened and, gradually, solvent shared and solvent separated structures are expected to become populated.

As a model system for studying salt bridge formation and subsequent weakening upon sequential hydration, we chose the terminated lysine-glutamate (Ac-Lys-Glu-NHMe) dipeptide. The choice of Glu rather than Asp as an acidic residue is motivated by the fact that its longer chain is more flexible. The choice of Lys rather than Arg as a basic residue has been made since the former has only one geometric way to form a salt bridge. Note that the capped (neutral) termini are chosen to reduce the complexity of potential proton transfer patterns, thus allowing us to focus solely on the salt bridge formation upon microhydration. Methodologically, the current work combines *ab initio* density functional theory (DFT) molecular dynamics for the description of the proton transfer during formation of the salt bridge with classical molecular dynamics focusing on the process of weakening of the salt bridge upon increasing hydration. This approach allows us to characterize and quantify the stability of the salt bridge as a function of the degree of its hydration with consequences for salt bridge stabilities in proteins.

## II. METHODS

### A. Born-Oppenheimer molecular dynamics

The focus of the first part of the present paper is on the proton transfer between Lys and Glu which cannot be studied using empirical force fields assuming a fixed protonation state of all amino acid side chains. Hence, we opt for *ab initio* Born-Oppenheimer molecular dynamics (BOMD) simulations, where the underlying forces are obtained from electronic structure calculations performed every time step. Using the open source computer program CP2K with its hybrid Gaussian and plane-wave approach,<sup>20</sup> the electrons are treated at the DFT level of theory using the Becke-Lee-Young-Parr (BLYP) functional<sup>21,22</sup> to which dispersion interactions are added using the Grimme correction scheme.<sup>23</sup> An atom-centered triple- $\zeta$  Gaussian basis set augmented with two polarization functions (TZV2P MOLOPT)<sup>24</sup> is used and the Goedecker-Teter-Hutter norm-conserving pseudopotentials<sup>25</sup> are employed to replace the core electrons of the heavier atoms (C, O, and N). A cutoff of 280 Ry is used for the auxiliary plane waves basis set. Depending on the number of water molecules, the length of the edge of the cubic unit cell varies between 1.8 and 2.2 nm, with the Poisson equation being solved with a wavelet solver<sup>26</sup> with open boundary conditions which are adequate for the isolated microhydration systems investigated here. In order to check the accuracy of the employed DFT method, we compared selected energy profiles to results obtained by BLYP, B3LYP, and MP2 methods and all-electron basis sets (6-31+g\*, 6-31++g\*, and aug-cc-pVDZ) as implemented in the GAUSSIAN software package,<sup>27</sup> see Figs. S1 and S2.<sup>28</sup>

In modeling the dynamics of the intra-molecular proton transfer with the above-mentioned simulation technique, we run BOMD trajectories integrating the equations of motion with a time step of 0.5 fs. A constant temperature of

300 K was maintained using the canonical sampling through velocity rescaling (CSVR) thermostat<sup>29</sup> with a time constant of 50 fs. We focused mainly on smaller clusters containing up to 5 water molecules where we ran 58 trajectories of up to 20 ps length. However, in a few cases we also simulated clusters with up to 64 water molecules solvating the dipeptide.

### B. Classical molecular dynamics

For clusters containing more than 100 water molecules, which are incidentally not yet enough to completely solvate the dipeptide investigated here, BOMD simulations are becoming computationally prohibitively expensive. Therefore, for larger systems we switch to classical molecular dynamics simulations with empirical force fields. This can be justified for situations where the zwitterionic protonation state of the amino acid side chains does not change anymore to the neutral state, which is the case for all of BOMD simulations with more than 10 water molecules as we shall demonstrate below. To simulate clusters with up to 1000 water molecules as well as the dipeptide in bulk water, we used the OPLS-AA force field<sup>30,31</sup> as implemented in the GROMACS software,<sup>32</sup> together with the TIP4P water model.<sup>33</sup> The geometry of water molecules was kept rigid using the SETTLE algorithm,<sup>34</sup> while all other bonds containing hydrogen were constrained to standard bond lengths by the LINCS algorithm.<sup>35</sup> The equations of motion were integrated using the leap-frog algorithm with a time step of 1 fs. Simulations were performed at the constant temperature of 300 K employing the CSVR thermostat<sup>29</sup> with the time constant of 0.5 ps. In cluster simulations all the electrostatic and van der Waals pair interactions were summed up. In bulk simulations of a 3 nm cubic unit cell containing 859 water molecules with periodic boundary conditions an atmospheric pressure of 1 bar was maintained by the Berendsen barostat<sup>36</sup> with the coupling constant of 0.5 ps. To treat long-range electrostatic interactions the particle mesh Ewald method<sup>37</sup> was used. Both short-range electrostatic and van der Waals interactions were truncated at 1.2 nm.

A common problem in simulations of clusters at ambient temperature with open boundary conditions is that water molecules evaporate from the cluster surface which typically occurs on a 100 ps time scale at room temperature. While this does not affect our BOMD simulations where the trajectories are much shorter, care has to be taken to avoid evaporation in our longer classical MD simulations. We attach each of the water molecules to an immobile dummy atom with zero mass and no interaction parameters by a restraining potential which is zero below a distance  $r_W$  and which is harmonic with a force constant  $k_W$  for longer distances. In addition, also the midpoint between the charged side chain termini is restrained through a harmonic potential to the central dummy atom to ensure more symmetric solvation of the side chains.

The choice of the restraint constants is closely connected to the choice of the initial conditions for cluster simulations with  $n$  water molecules: From an equilibrated bulk simulation we pick one of the instances with a closed salt bridge (contact ion pair). Then the radius of the sphere that circumscribes the  $n$  molecules closest to the midpoint of the ion pair augmented by 0.1 nm is used to define the restraint radius  $r_W$ . The

corresponding force constant  $k_W$  is set to  $10^4$  kJ mol<sup>-1</sup> nm<sup>-2</sup> while the restraining force constant for the midpoint of the side chain ion pair is chosen to be  $10^3$  kJ mol<sup>-1</sup> nm<sup>-2</sup>. The results do not change significantly if the restraint radius  $r_W$  and force constant  $k_W$  are varied in reasonable margins. For more details see Fig. S3.<sup>28</sup>

In addition to direct MD simulations, free energy profiles for salt bridge opening (i.e., increasing the C...N distance  $r_{CN}$ ) are obtained by umbrella sampling. Sampling windows equally spaced by 50 pm with harmonic umbrella potentials with a force constant of  $10^3$  kJ mol<sup>-1</sup> nm<sup>-2</sup> were used. At  $r_{CN} = 0.45$  nm, where the barrier is located, simulation with umbrella potential with force constant of  $2 \times 10^3 - 4 \times 10^3$  kJ mol<sup>-1</sup> nm<sup>-2</sup>, depending on the cluster size, ensures denser sampling (overlap of histograms). The weighted histogram analysis method<sup>38</sup> as implemented in GROMACS<sup>39</sup> is employed to extract a free energy profile from these histograms. Finally, free energy profiles are corrected by a volume entropy factor  $k_B T \ln(4\pi(r_{CN}/r_0)^2)$  and shifted so that the minimum value equals zero.

### III. RESULTS AND DISCUSSION

#### A. Dynamics of proton transfer between side chains

In this section we investigate the interplay between the neutral and zwitterionic states of the Ac-Lys-Glu-NHMe dipeptide focusing mainly on small clusters with up to  $n = 5$  water molecules. We employ the BOMD simulation technique introduced in Sec. II A, which allows us to study dynamics of proton transfer as a function of the number of water molecules involved. Figure 1 shows the capped model dipeptide with the atom labeling that is used throughout this text. A hydrogen bond can be formed in the salt bridge between NH<sub>2</sub> in Lys and one of the carboxylic oxygen atoms O1 or O2 in Glu. In addition, the three backbone carbonyl oxygen atoms (Obac1–3) are potential hydrogen bond acceptors, while three backbone amide hydrogen atoms (Hbac1–3) are potential donors. This results in a large number of local minima on the potential

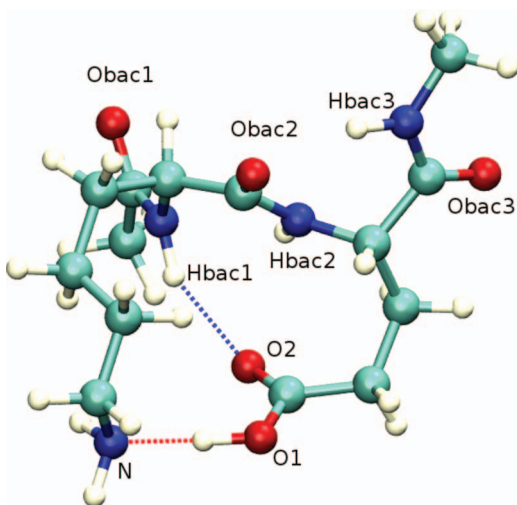


FIG. 1. Atom labeling of the Ac-Lys-Glu-NHMe model peptide, restricted just to groups that can form hydrogen bonds.

energy surface even for the systems with a small number (or even no) water molecules.

As a first step we selected several minimum energy conformations where the side chain termini are in contact with each other and performed unrelaxed scans of the potential energy surface, i.e., moving the proton along a straight line between amino N in Lys and one carboxylic O in Glu with all other atoms fixed. Our DFT calculations in the CP2K setup slightly overestimate the stability of the neutral form in comparison with higher level methods with all-electron basis sets, but the energetic order of the different protonation states as well as the shapes of the energy profiles remain unchanged (for more details on benchmarking see Fig. S2<sup>28</sup>).

While these scans serve as a preliminary survey of the proton transfer energetics, a more complete picture including water rearrangements and conformational dynamics of the peptide is provided by sampling the conformational space with BOMD trajectories. For this purpose, initial conditions are obtained by minimization of BLYP or OPLS-AA energies or are taken from snapshots of classical molecular dynamic simulations. The bare dipeptide, when starting from its neutral state, remains in that state over the duration of our simulations. If, however, a zwitterionic state is initially prepared, the proton hops back on a sub-picosecond time scale, once the charged side chains get close enough to each other. Note that the preparation of this zwitterionic initial condition requires the amino group to form a hydrogen bond with the backbone (Obac2). In addition, formation of 7-membered rings with hydrogen bonds between backbone atoms Hbac3 and Obac2 or between Obac1 and Hbac2, or a 10-membered ring with a hydrogen bond between Hbac3 and Obac1 is often observed.

The effect of attaching water molecules to the dipeptide is discussed with emphasis on structural motifs as shown in Fig. 2. A *contact neutral* state (Fig. 2(a)) with a transferable proton at O1 represents a typical arrangement for clusters with one or two water molecules, where one water molecule usually forms a bridge between O2 (the oxygen atom closer to the backbone) and NH<sub>2</sub> or Hbac1, 2. The second water molecule can be bound either to the backbone or to the first one. These initial conditions not only remain stable for the time span of our simulation, but also, when starting a BOMD trajectory from a contact zwitterion with the proton located between the amino group and the O1 atom, the proton is directly transferred to O1 (neutral state). This proton hop is related to the weakening of additional hydrogen bonds involving the water molecule and/or the backbone. For a larger number of water molecules ( $n \geq 3$ ) such neutral arrangements are stable only if the water molecules are mainly involved in hydrogen bonds within themselves rather than with the side chain termini, but this is rarely observed. Neutral structures with a transferable proton at O2 are also possible in case of one and two water molecules attached. In this arrangement, it is easier to form hydrogen bonds between side chain termini and the backbone and water molecules at the same time. However, this favors the zwitterionic state and that is probably why we did not observe such neutral structure for a larger number of water molecules.

Finally, a *solvent shared neutral* state of the dipeptide is also found, see Fig. 2(b). This state is stable on the time



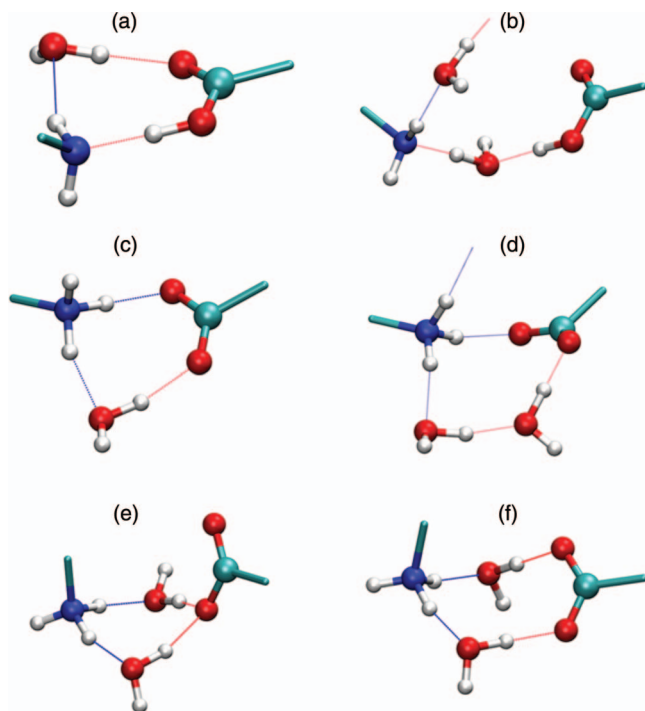


FIG. 2. Details of the model peptide Ac-Lys-Glu-NHMe side chain termini. Top: Dipeptide in neutral form with one (left: contact) and with two water (right: solvent shared) molecules attached. Center: Zwitterionic contact pair with one (left) or two (right) water molecules attached. Bottom: Solvent shared ion pairs involving one (left) or two (right) oxygen atoms of the carboxyl group.

scale of our simulations (20 ps) in case of one or two water molecules, since they can form water bridges between these polar groups, and being neutral, they do not directly attract each other too strongly. In case of three water molecules, formation of a solvent shared zwitterion (Fig. 2(e)) from a solvent shared neutral initial condition (Fig. 2(b)) is also observed, in which case the proton is transferred through a water bridge.

Already the addition of a single water molecule can stabilize a *zwitterionic* state for several tens of ps if additional stabilization from the backbone is provided, see Fig. 2(c), (for more details see also Figs. S1(c) and S1(d)<sup>28</sup>). If the transferable proton originates from the oxygen that is closer to the backbone (O2), frequent transitions between neutral and zwitterionic form are observed, with the additional condition that the water molecule is placed between the other amino hydrogen and the O1 atom. Under these circumstances, the salt bridge can be stabilized by up to three hydrogen bonds, two from the water molecule and one from the backbone, which appears sufficient to stabilize the charged groups. In one case, in addition to the previously described stabilization, there we observed a hydrogen bond formed between amino hydrogen and Obac2 which leads to up to 4 stabilizing hydrogen bonds and no proton transfer leading back to the neutral state occurs.

With two water molecules, when the *contact zwitterion* is initially prepared with the proton between the amino group and the O2 atom, we observe two arrangements with sufficient number of hydrogen bonds to stabilize the zwitterionic state of the side chains with one or two water molecules between the amino group and the O1 atom (Figs. 2(c) and 2(d)). In

the former case, the other water molecule is bound to O2, in the later case, O2 is stabilized by hydrogen bond from backbone. With three water molecules, there are more possibilities for the salt bridge to stay zwitterionic on the time scale of our simulations and for four water molecules, the dipeptide is mainly found in this symmetrically solvated zwitterionic state.

In principle, a cluster of the peptide with two water molecules is the smallest system to accommodate a *solvent shared zwitterionic* state. However, such an initial condition is not stable and within few ps it develops in the following two ways: either the proton can be transferred through a water bridge to Glu or the charges come closer to each other to form a contact ion pair with the proton between N and O1 and then the proton is transferred to Glu. In case of three water molecules, the conversion from a solvent shared zwitterionic initial state (Figs. 2(e) and 2(f)) to a contact ion pair (salt bridge) is also possible, if the resulting structure provides a sufficient number of hydrogen bonds. If, however, during this conversion from a solvent shared state to a contact ion pair a water molecule leaves its binding site, the system proceeds toward formation of a tight neutral state.

In several simulations with four water molecules attached, the formation of a solvent shared ion pair from an initial contact ion pair is observed, but after less than 1 ps this is converted back to a contact pair. For clusters with five water molecules there are no new qualitative features in comparison with the situation with four waters.

Building on the above case studies, general features of the proton transfer reaction mechanism between Glu and Lys side chains can be discussed, focusing on the question under which circumstances a proton can be transferred. We introduce an asymmetry variable  $\delta = r_{XH} - r_{YH}$  for the motion of a proton between two heavier atoms labeled as X and Y.<sup>40</sup> A general feature observed in most of our reactive BOMD trajectories is illustrated in Fig. 3 for the example of a selected Ac-Lys-Glu-NHMe(H<sub>2</sub>O)<sub>2</sub> trajectory: For a direct pro-

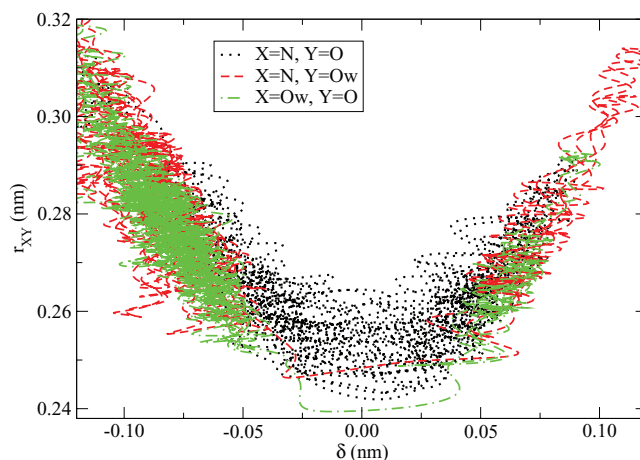


FIG. 3. Proton transfer mechanisms from a 4 ps part of a BOMD trajectory for Ac-Lys-Glu-NHMe(H<sub>2</sub>O)<sub>2</sub>. The figure shows the heavy-heavy atom distance vs. the corresponding proton asymmetry variable  $\delta$  (see text) for three different transfer scenarios: Proton transferred between amino nitrogen and carboxylic oxygen (black) or water oxygen (red), or between amino water and carboxylic oxygen (green).

ton transfer to occur between N(=X) and O(=Y) the NO distance must be smaller than 0.265 nm while for a transfer through a bridge of a single water molecule the corresponding NOW distance must be less than 0.255 nm and the OwO distance even below 0.245 nm. The figure also shows that the direct proton transfer occurs much more frequently than the indirect one through the water bridge, which has been observed only once within the duration of our trajectory.

In addition to the appropriate configuration of the X and Y heavy atom sites, we already mentioned above the crucial role of additional hydrogen bonds in promoting the proton transfer reactions. By additional hydrogen bonds we mean those in which side chain termini are directly involved, but not the hydrogen bond between amino group and carboxylic group in contact arrangement or those involving a water molecule which serves as a bridge in the solvent shared arrangement. Instead of using discrete cut-off criteria for the donor-acceptor distance ( $r$ ) and angle ( $\alpha$ ), we use for the analysis a smeared non-integer number of hydrogen bonds  $N_{\text{HB}}$  in order to smooth out discrete jumps in hydrogen bonding numbers,

$$N_{\text{HB}} = 0.25 \operatorname{erfc} \left( \frac{r - r_0}{\sqrt{2}\sigma_r} \right) \operatorname{erfc} \left( \frac{\alpha - \alpha_0}{\sqrt{2}\sigma_\alpha} \right), \quad (1)$$

where  $r_0 = 0.35$  nm,  $\sigma_r = 25$  pm,  $\alpha_0 = 30^\circ$ , and  $\sigma_\alpha = 5^\circ$ . A typical BOMD result for a proton transfer trajectory (with one water molecule in this case) is displayed in Fig. 4. The asymmetry variable indicates whether the system is neutral ( $\delta > 0$ ) or zwitterionic ( $\delta < 0$ ) and it shows strong correlation with the smoothed number of additional hydrogen bonds. For less than two hydrogen bonds, the peptide is almost always in its neutral state. If the number of hydrogen bonds is between two and three, there is a dynamical equilibrium between the neutral and the zwitterionic state. Finally, when the number of additional H-bonds exceeds three, the zwitterionic state is stabilized without the proton moving back to Glu. Given this correlation between the proton transfer reaction and the number of additional hydrogen bonds, it is of interest to study the time delay between changes of these two quantities. For most of the proton transfer reactions from the neutral to the zwitteri-

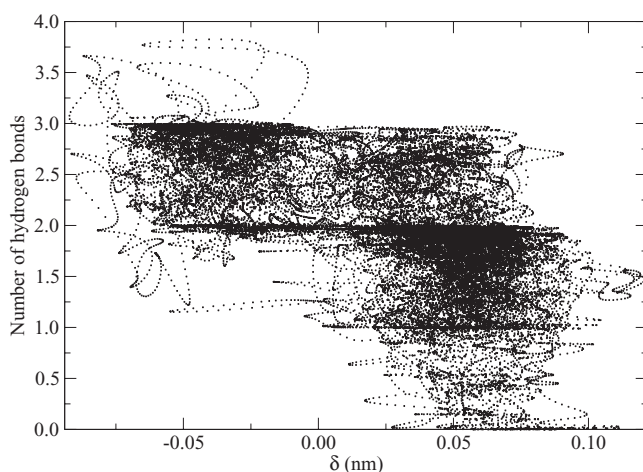


FIG. 4. Smeared number of hydrogen bonds additionally stabilizing the side chain termini and proton asymmetry coordinate  $\delta = r_{\text{NH}} - r_{\text{OH}}$ .

onic state, it is observed that the number of H-bonds increases (exceeds two)  $\sim 50$  fs before the proton hop, indicating that it is triggered by the solvent and/or backbone dynamics. Vice versa, it is found that for conversions from zwitterionic to neutral state the number of hydrogen bonds decreases some  $\sim 40$  fs afterwards, because neutral side chain termini are less attractive for water molecules than charged ones. The specific numbers are of course somewhat definition dependent.

## B. Dynamics of opening and closing the salt bridge

In the following, we extend our study of sequential hydration of the Ac-Lys-Glu-NHMe dipeptide toward much larger clusters, eventually approaching the bulk limit. Since the BOMD simulation has shown that only the zwitterionic state is populated if more than 10 water molecules are attached, the stability of that protonation state can be safely assumed in simulations of these larger systems. This allows us to disregard potential proton transfer and, therefore, to switch to classical molecular dynamics with an empirical (OPLS-TIP4P) force field for the remainder of this work. For clusters of increasing size (from 20 to 1000 water molecules) a series of MD simulations of 200 ns duration each were performed at 300 K, as described in Sec. II B.

To investigate the opening and closing of the salt bridge, we focus on the distribution of the  $\text{COO}^- \cdots \text{NH}_3^+$  side chain termini distances ( $r_{\text{CN}}$ ) obtained directly from these simulations as presented in Fig. 5. For 20 water molecules, the  $r_{\text{CN}}$  distance is practically all the time below 0.4 nm, which indicates the dominance of a salt bridge (contact ion pair) for this cluster size. For 30 water molecules, we start observing significant occurrence of  $r_{\text{CN}}$  values around 0.55 nm, i.e., formation of a solvent shared ion pair. When 40 or more water

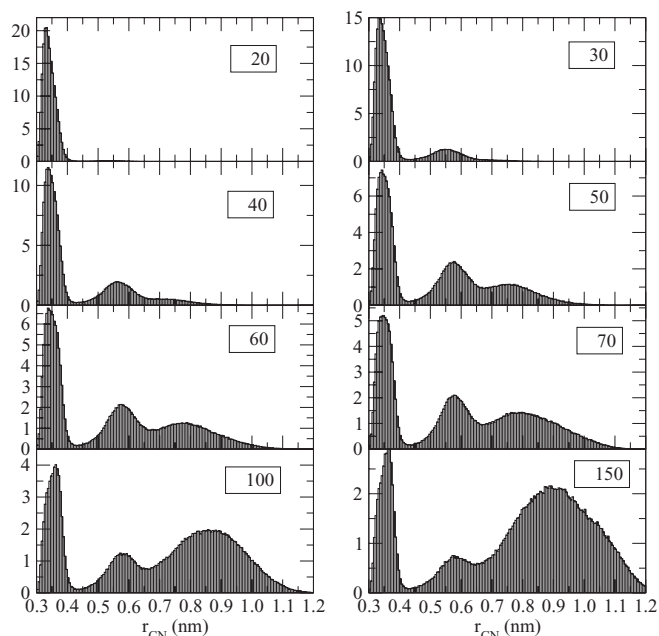


FIG. 5. Normalized distributions of CN distances for the  $\text{COO}^- \cdots \text{NH}_3^+$  side chain termini from 200 ns/300 K simulation for Ac-Lys-Glu-NHMe dipeptide solvated in water clusters of different sizes.

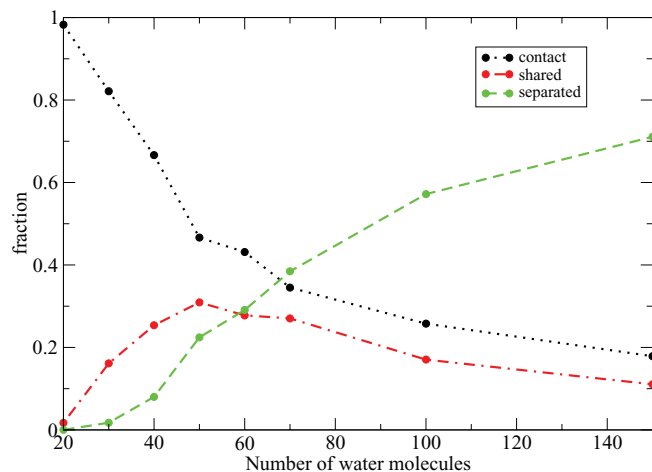


FIG. 6. Fractions of contact, solvent shared, and solvent separated ion pairs obtained from 200 ns/300 K direct MD simulations as a function of the number of water molecules attached to the Ac-Lys-Glu-NHMe dipeptide. Dashed lines serve to guide the eye.

molecules are attached to the model peptide, solvent separated ion pairs with two or more water layers between the charged species become populated.

The positions of the minima in the histograms in Fig. 5 are found near 0.43 nm and 0.67 nm regardless of the cluster sizes, defining operationally the boundaries between contact, solvent shared, and solvent separated ion pairs. Figure 6 shows how the distribution of these ion pairing motifs depends on the number of water molecules. While the fraction of contact ion pairs decreases monotonically with increasing cluster size, the fraction of solvent separated pairs increases and starts to dominate beyond 70 water molecules. At intermediate cluster sizes with 50 solvent molecules, the fraction of solvent shared ion pairs exhibits a maximum but it never becomes the dominant contribution.

Although the long direct MD simulations are appropriate for the above analysis of populations of contact, solvent shared or solvent separated ion pairs, the heights of the barriers separating them may be not calculated accurately enough by a simple Boltzmann inversion of the histograms of Fig. 5 (with the volume entropy correction applied). Hence, we used umbrella sampling,<sup>38</sup> as described in Sec. II B to obtain free energy profiles along the  $r_{\text{CN}}$  coordinate describing the opening and closing of the salt bridge.

We first performed test calculations employing a  $\text{NH}_4^+ \cdots \text{HCOO}^-$  ion pair rather than the whole dipeptide, excluding thus effects of the backbone and the aliphatic parts of the side chains. The free energy difference between contact and solvent shared  $\text{NH}_4^+ \cdots \text{HCOO}^-$  ion pairs, as well as the barrier between them, decrease monotonically with the number of water molecules added, see Fig. 7. The principal reason for this is the more complete hydration of the charges, which become increasingly dielectrically screened from each other. Convergence to the corresponding bulk values occurs around 100 water molecules for  $r_{\text{CN}} \leq 0.6$  nm.

Analogous free energy profiles for the salt bridge of the dipeptide in water are shown in Fig. 8. The barrier between contact and solvent shared ion pairs decreases with increas-

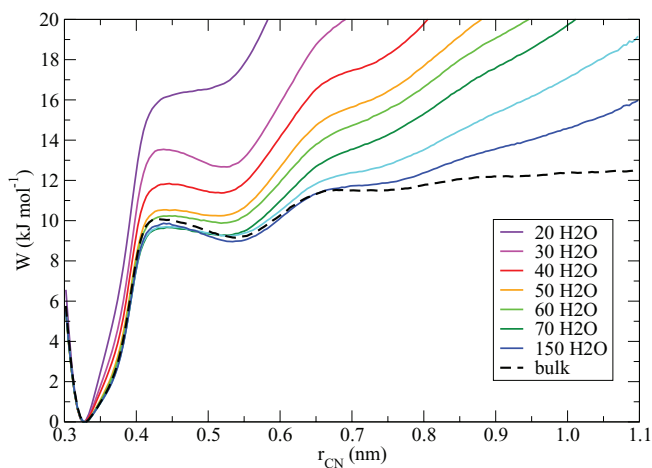


FIG. 7. Free energy profile of  $\text{NH}_4^+ \cdots \text{HCOO}^-$  ion pair dissociation in water clusters of different sizes obtained by umbrella sampling.

ing cluster size up to 150 water molecules, but for larger clusters it starts to increase again. The free energy difference between the two minima corresponding to contact and solvent shared ion pair decreases with increasing cluster size up to 600 water molecules, then increases again for 1000 water molecules, still not being fully converged to the bulk value. From about 70 water molecules onward, a solvent separated minimum appears, which becomes deeper and shifts toward larger distances with increasing cluster size. From about 150 water molecules it becomes deeper than the solvent shared one and it also becomes broader with increasing number of water molecules attached. Note that due to the finite length of side chains, the  $r_{\text{CN}}$  distance cannot exceed 1.3 nm.

The dependence of the dipeptide salt bridge free energy profile on cluster size is more complex than that for a free  $\text{NH}_4^+ \cdots \text{HCOO}^-$  ion pair. In addition to the trend resulting from hydration of charged groups, in the dipeptide there is also the preference of non-polar parts of the molecule to be close to the surface of the water droplet. For medium cluster sizes,  $\text{CH}_2$  groups of the aliphatic parts of the side chains can be exposed with charged side chain termini sufficiently hy-

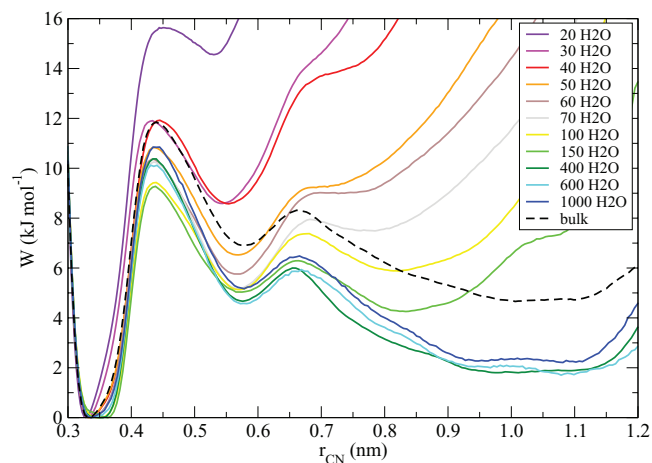


FIG. 8. Free energy profile of Ac-Lys-Glu-NHMe dipeptide salt bridge opening in water clusters of different sizes obtained by umbrella sampling.



TABLE I. Lifetimes (ps) from linear fitting of logarithm of probability of staying in particular state. The lifetime is calculated as  $\tau = -1/k$ , where  $k$  is the slope of the line, the shortest times were omitted from the fit in order to reduce the influence of recrossings. For details see Fig. S4.<sup>28</sup>

Number of water molecules	$\tau_{\text{contact}}$ (ps)	$\tau_{\text{shared}}$ (ps)	$\tau_{\text{separated}}$ (ps)
20	272	12	...
30	171	17	7
40	132	14	13
50	124	13	25
60	117	12	49
70	106	12	57
100	111	12	95
150	132	10	185

drated, which facilitates salt bridge opening compared to the situation in the bulk (or in very large clusters). Finally, the relatively pronounced solvent shared minimum is likely also due to the effect of configurational entropy, since in this arrangement the side chains can adopt more conformations than either for the contact pair or the completely stretched chains.

In order to estimate the lifetimes of contact, solvent shared, and solvent separated ion pairs in the dipeptide, we plotted in each case probability of staying in particular state as a function of time (for details see Fig. S4<sup>28</sup>) and fitted its logarithm by a straight line, the resulting lifetimes being summarized in Table I. The lifetime of the contact ion pair decreases from 270 ps to 170 ps upon increasing the number of water molecules from 20 to 30, and from 40 water molecules it levels off around 120 ps. The lifetime of the solvent shared ion pair is roughly ten times shorter (i.e., around 12 ps) for all cluster sizes, which correlates with low barriers toward both contact and solvent separated pairs. The lifetime of the solvent separated ion pair increases from roughly 10 ps for 40 water molecules to 50 ps for cluster size of 60 and then further to 100 ps for clusters containing about 100 water molecules. For the cluster containing 150 water molecules, however the decay is not perfectly exponential, so that the estimate of lifetime of 180 ps is less reliable.

#### IV. CONCLUSIONS

We investigated the formation and stability of a lysine-glutamate salt bridge upon sequential addition of water molecules. Proton transfer connecting neutral and zwitterionic states of the Ac-Lys-Glu-NHMe model peptide in small clusters with up to 5 water molecules was described employing DFT-based BOMD simulations. While the bare peptide prefers to be in its neutral state, proton transfer from Glu to Lys, leading to a zwitterionic salt bridge state as a contact ion pair, is found already when a single water molecule is added. Solvent shared ion pairs are found from four water molecules onwards, but with lifetimes limited to a picosecond at room temperature. In all the *ab initio* molecular dynamics studies it is found that the microsolvated zwitterion can only exist if the pair of ions—in addition to their mutual attraction—is stabilized by at least three further hydrogen bonds involving the hydrating water molecules and possibly the peptide backbone. The formation of a zwitterionic state from a neutral one is trig-

gered by the increase of the number of extra hydrogen bonding interactions, whereas the reversed proton transfer triggers the reduction of the number of these hydrogen bonds.

Beyond a cluster size of 10 water molecules the model dipeptide is always found in its zwitterionic state. By virtue of classical MD simulations the onset of long-lived solvent shared ion pairs is observed for  $\sim 30$  water molecules (occasional opening of the salt bridge starts already for smaller systems, albeit somewhat larger in classical MD compared to BOMD) while solvent separated ion pairs (with two or more water layers between the charges) are found when 40 or more water molecules are attached to the model peptide. In case of the simple  $\text{NH}_4^+ \cdots \text{HCOO}^-$  ion pair, umbrella sampling calculations show that the free energy difference between contact and solvent shared ion pairs, as well as the barrier between them, decrease monotonically with the number of water molecules added. However, the dependence of the free energy profile for dipeptide salt bridge opening on the number of hydrating water molecules is more complex, due to the influence of configurational entropy and preference of less polar parts of the molecule for the surface of the cluster. The lifetime of the contact ion pair of the model dipeptide in a cluster containing more than 40 water molecules is estimated to be 120 ps, the solvent shared ion pair lives about ten times shorter and the lifetime of the solvent separated ion pair increases from about 10 ps for the cluster containing 40 water molecules to almost 200 ps for the cluster containing 150 water molecules.

Our detailed study, showing first the formation and then subsequent weakening of a salt bridge upon increasing the number of hydrating water molecules has implications for the stability of salt bridges in hydrated proteins. Indeed, it has been shown that strong salt bridges form when charged residues are partially buried from surfaces of proteins.<sup>10</sup> In conclusion, our work indicates that neither too little nor too much hydration is beneficial for a salt bridge, which tends to be most stable upon moderately dehydrated conditions, such as in concave pockets at protein surfaces.

#### ACKNOWLEDGMENTS

This work was made possible through generous grants of computer time at The North-German Supercomputing Alliance (HLRN). E.P. and O.M. acknowledge support from the International Max Planck Research School on Dynamical Processes in Atoms, Molecules, and Solids. P.J. thanks to Czech Science Foundation (Grant No. P208/12/G016) and acknowledges the Praemium Academie award from the Czech Academy of Sciences for support.

<sup>1</sup>S. Kumar and R. Nussinov, *ChemBioChem* **3**, 604 (2002).

<sup>2</sup>C. D. Waldburger, J. F. Schildbach, and R. T. Sauer, *Nat. Struct. Biol.* **2**, 122 (1995).

<sup>3</sup>W. C. Wimley, K. Gawrisch, T. P. Creamer, and S. H. White, *Proc. Natl. Acad. Sci. U.S.A.* **93**, 2985 (1996).

<sup>4</sup>A. Horovitz, L. Serrano, B. Avron, M. Bycroft, and A. R. Fersht, *J. Mol. Biol.* **216**, 1031 (1990).

<sup>5</sup>J. M. Scholtz, H. Qian, V. H. Robbins, and R. L. Baldwin, *Biochemistry* **32**, 9668 (1993).

<sup>6</sup>S. Kumar and R. Nussinov, *J. Mol. Biol.* **293**, 1241 (1999).

<sup>7</sup>Z. S. Hendsch and B. Tidor, *Protein Sci.* **3**, 211 (1994).

<sup>8</sup>H. Gong and K. F. Freed, *Biophys. J.* **98**, 470 (2010).

- <sup>9</sup>A. Masunov and T. Lazaridis, *J. Am. Chem. Soc.* **125**, 1722 (2003).
- <sup>10</sup>J. Bush and G. I. Makhatadze, *Proteins* **79**, 2027 (2011).
- <sup>11</sup>T. Kajander, P. C. Kahn, S. H. Passila, D. S. Cohen, L. Lehtio, W. Adolfsen, J. Warwicker, U. Schell, and A. Goldman, *Structure (London)* **8**, 1203 (2000).
- <sup>12</sup>M. R. Gunner, M. A. Saleh, E. Cross, A. ud-Doula, and M. Wise, *Biophys. J.* **78**, 1126 (2000).
- <sup>13</sup>D. G. Isom, B. R. Canon, C. A. Castaneda, A. Robinson, and B. E. Garcia-Moreno, *Proc. Natl. Acad. Sci. U.S.A.* **105**, 17784 (2008).
- <sup>14</sup>M. N. Blom, I. Compagnon, N. C. Polfer, G. V. Helden, G. Meijer, S. Suhai, B. Paizs, and J. Oomens, *J. Phys. Chem. A* **111**, 7309 (2007).
- <sup>15</sup>A. Fernandez-Ramos, Z. Smedarchina, W. Siebrand, and M. Z. Zgierski, *J. Chem. Phys.* **113**, 9714 (2000).
- <sup>16</sup>E. Kassab, J. Langlet, E. Evleth, and Y. Akacem, *J. Mol. Struct.: THEOCHEM* **531**, 267 (2000).
- <sup>17</sup>R. Ramaekers, J. Pajak, B. Lambie, and G. Maes, *J. Chem. Phys.* **120**, 4182 (2004).
- <sup>18</sup>S. Xu, J. M. Nilles, and K. H. Bowen, *J. Chem. Phys.* **119**, 10696 (2003).
- <sup>19</sup>K. Leung and S. B. Rempe, *J. Chem. Phys.* **122**, 184506 (2005).
- <sup>20</sup>J. VandeVondele, M. Krack, F. Mohamed, M. Parrinello, T. Chassaing, and J. Hutter, *Comput. Phys. Commun.* **167**, 103 (2005).
- <sup>21</sup>A. D. Becke, *Phys. Rev. A* **38**, 3098 (1988).
- <sup>22</sup>C. Lee, W. Yang, and R. G. Parr, *Phys. Rev. B* **37**, 785 (1988).
- <sup>23</sup>S. Grimme, *J. Comput. Chem.* **27**, 1787 (2006).
- <sup>24</sup>J. VandeVondele and J. Hutter, *J. Chem. Phys.* **127**, 114105 (2007).
- <sup>25</sup>S. Goedecker, M. Teter, and J. Hutter, *Phys. Rev. B* **54**, 1703 (1996).
- <sup>26</sup>L. Genovese, T. Deutsch, A. Neelov, S. Goedecker, and G. Beylkin, *J. Chem. Phys.* **125**, 074105 (2006).
- <sup>27</sup>M. J. Frisch, G. W. Trucks, H. B. Schlegel, *et al.*, GAUSSIAN 09, Revision A.01, Gaussian, Inc., Wallingford, CT, 2009.
- <sup>28</sup>See supplementary material at <http://dx.doi.org/10.1063/1.4765052> for benchmark calculations and figures of lifetimes of contact, solvent shared, and solvent separated ion pairs.
- <sup>29</sup>G. Bussi, D. Donadio, and M. Parrinello, *J. Chem. Phys.* **126**, 014101 (2007).
- <sup>30</sup>W. L. Jorgensen, D. S. Maxwell, and J. Tirado-Rives, *J. Am. Chem. Soc.* **118**, 11225 (1996).
- <sup>31</sup>G. A. Kaminski, R. A. Friesner, J. Tirado-Rives, and W. L. Jorgensen, *J. Phys. Chem. B* **105**, 6474 (2001).
- <sup>32</sup>B. Hess, C. Kutzner, D. van der Spoel, and E. Lindahl, *J. Chem. Theory Comput.* **4**, 435 (2008).
- <sup>33</sup>W. L. Jorgensen, J. Chandrasekhar, J. D. Madura, R. W. Impey, and M. L. Klein, *J. Chem. Phys.* **79**, 926 (1983).
- <sup>34</sup>S. Miyamoto and P. A. Kollman, *J. Comput. Chem.* **13**, 952 (1992).
- <sup>35</sup>B. Hess, H. Bekker, H. J. C. Berendsen, and J. G. E. M. Fraaije, *J. Comput. Chem.* **18**, 1463 (1997).
- <sup>36</sup>H. J. C. Berendsen, J. P. M. Postma, W. F. van Gunsteren, A. DiNola, and J. R. Haak, *J. Chem. Phys.* **81**, 3684 (1984).
- <sup>37</sup>U. Essmann, L. Perera, M. L. Berkowitz, T. Darden, H. Lee, and L. G. Pedersen, *J. Chem. Phys.* **103**, 8577 (1995).
- <sup>38</sup>S. Kumar, J. M. Rosenberg, D. Bouzida, R. H. Swendsen, and P. A. Kollman, *J. Comput. Chem.* **13**, 1011 (1992).
- <sup>39</sup>J. S. Hub, B. L. de Groot, and D. van der Spoel, *J. Chem. Theory Comput.* **6**, 3713 (2010).
- <sup>40</sup>M. E. Tuckerman, *Science* **275**, 817 (1997).